Phase transitions and electron-induced rearrangements in adsorbed hydrogen and deuterium films on Mo(011)

V. V. Gonchar, O. V. Kanash, I. A. Kotlyarova, A. G. Fedorus, and A. F. Fedosenko

Institute of Physics of the Academy of Sciences of the Ukrainian SSR

The atomic structure of hydrogen and deuterium films adsorbed on Mo(011) is investigated by the low-energy electron diffraction technique over a broad temperature range ($T = 5$–300 K) and coverage $\vartheta = 0$–1. The phase diagram of the H–Mo(011) system with a single ordered structure (2×2) is determined for a stoichiometric coverage $\vartheta = 0.5$. Thermally-activated migration of the adsorbed atoms is found to be substantial at $T > 20$ K. The order-disorder transitions for the (2×2) structure were investigated by analyzing the temperature dependence of the structural reflection intensities: The critical exponent $\beta = 0.25 \pm 0.07$ of the order parameter is found. The effect of slow electrons on the degree of structural perfection of films in a nonequilibrium (frozen at $T = 5$ K) state is analyzed. The degree of order of initially perfect structures (pre-annealed films) diminishes under electron beam action; electron-induced (EI) disorder is not complete, but rather ceases at some nonzero level. The electron-induced disorder cross section is estimated at $\sigma_{EID} \sim 10^{-18}$ cm^2. Electron-induced ordering is found for films having a near-amorphous initial structure (obtained by low-temperature adsorption); such ordering is achieved with a stoichiometric coverage of the same final level at which electron-induced disordering ceases. The regularities of electron-induced disordering are analyzed. An isotopic effect is discovered (the process occurs five times slower in deuterium films). The rate of the process is found to have a weak dependence on electron energy and no threshold with respect to kinetic energy. The electron-induced rearrangement mechanism is discussed based on a hypothesis that the adsorbed atoms are excited by the electrons to the long-lived, above-barrier states (above the surface migration barrier).

INTRODUCTION

Interest in low-temperature studies of adsorbed hydrogen films can be attributed to recent reports of an anomalously high mobility of adsorbed hydrogen atoms on the (011) face of W at $T < 120$ K.[1–4] These studies analyzed fluctuations in the field-emission current at various temperatures to determine the existence of tunnel migration of the adsorbed atoms. The hypothesis of adsorbed hydrogen atom tunneling on the W surface was not, however, confirmed in many experiments using other techniques (the low-energy electron diffraction (LEED) technique[5] and surface reflection of conduction electrons[6]). On the other hand it has been established that the anomalous mobility of low-mass adsorbed atoms at low temperatures may be the result of low-energy electron action that in the final analysis causes electron-induced (EI) disordering of the adsorbed films.[5,7,8]

EI disordering is manifested as a reduction in the intensity of LEED reflections from the film structure at $T = 5$ K when a film that is pre-ordered by annealing is exposed to an electron beam. It was established that structures do exist [specifically, W(011)–$p(2 \times 1)$H] in which EI disordering is not completed, but rather stops at a specific level.[5] This served as the basis for the hypothesis of a competing EI ordering process, and direct observation of such a competing process is one of the primary goals of the present study. For this purpose it was necessary to fabricate films with a less-ordered structure than that obtained as a result of electron-induced disordering. In principle this can be attained by low-temperature adsorption of hydrogen. However this gas reaches the surface in the molecular phase, and the adsorbed particles may dissociate in the subsequent experiment,

thereby complicating interpretation of results. In order to avoid such a difficulty it is best to use a substrate where dissociation will occur during the adsorption process itself. A Mo(011) face was used as the substrate for this purpose; hydrogen is adsorbed by dissociation on this face as reported by Ref. 9. Preliminary results from an investigation of hydrogen isotope films (^{1}H on Mo(011)) were published in short form in Ref. 10. The present study reports data for the ^{1}H and ^{2}H isotopes.

The other purpose of the study was to investigate the order-disorder transitions and to obtain information on the critical exponent β of the order parameter. These data are of interest in connection with the unique behavior of the exponent β for the H–W(011) system: The two-fold difference for lattices described by a Hamiltonian of the same symmetry[11]. A (2×2) film structure of identical symmetry is typical of the H–Mo(011) system under analysis here. The phase diagram of the H–Mo(011) system is of independent interest. Reference 12 contains information on the phase diagram of this system, based on measurements of the width of the LEED reflections. The phase diagram is determined by a different technique[11] and over a broader temperature range in the present study.

EXPERIMENTAL TECHNIQUE

A "Reber" universal ultra-high vacuum set designed for comprehensive analysis of surface properties was used in the experiment. Figure 1 clearly demonstrates the methodological capabilities of the set. The following set modules were used in the study (including several nonstandard modules): A cryomanipulator, a low-voltage electron diffractometer with a telescopic spot-photometer (for LEED anal-
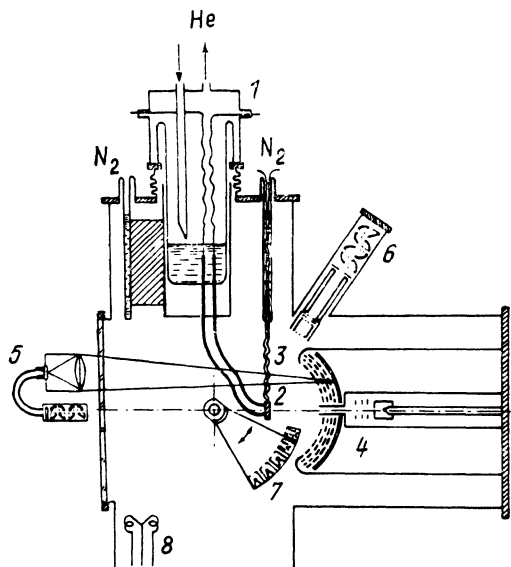
FIG. 1. Experimental setup: 1—Cryomanipulator; 2—specimen; 3—thermocouple; 4—low-voltage electron diffractometer; 5—telescopic spot-photometer; 6—quadrupole resonance mass-spectrometer; 7—rotating collar; 8—hydrogen and deuterium sources.
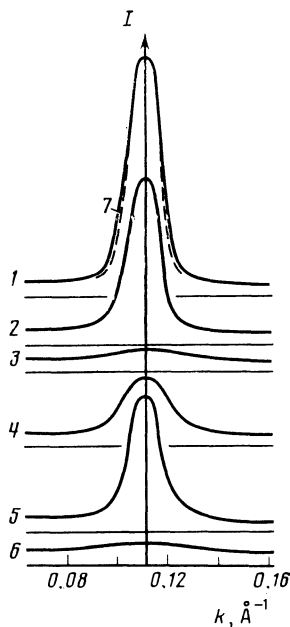

FIG. 2. Reflection profiles (1/2, 1/2) of a $(2 \times 2)_2$ deuterium structure for $\vartheta = 0.5$ and $E = 20$ eV corresponding to different film states: 1—$T = 5$ K after annealing at $T_{ann} = 300$ K, $t_{ann} = 10$ s; 2—$T = 5$ K after EI disordering, electron irradiation dosage: $J_c t = 0.15$ A·cm^{-2}·s; 3—$T = 5$ K after adsorption at $T_a = 5$ K; 4—the same film after EI ordering $(J_c t = 0.15$ A·cm^{-2}·s; 5—$T = 160$ K (the order-disorder transition points lie below T_c); 6—$T = 200$ K (in the vicinity of T_c); 7—curve 1 corrected for equipment distortion.

ysis of the surface structu·e), a quadrupole resonance mass-spectrometer (for mc 'oring gas composition and recording the thermal desorp'.ion spectra from the electron gun shot), a rotating collar containing two electron guns (one gun is used to irradiate the samples with a broad electron beam of variable energy, while the second is used to measure the contact potential difference by the Anderson method).

One necessary condition of EI rearrangement experiments is deep cooling of the specimen to avoid self-annealing of the film structure. The specimen was spot welded onto a direct-channel tungsten heater mounted on the molybdenum current taps of the cryomanipulator. Electron bombardment of the back end of the specimen can be used for additional heating (to $T \approx 2300$ K). When the cryomanipulator bath is filled with liquid helium the temperature of the specimen can be reduced to $T \approx 5$ K via heat dissipation through the specimen holder mount. The specimen temperature was measured by a thermocouple fabricated from VR-5/VR-20 alloys; liquid nitrogen is used for temperature control for the thermocouple ends.

Information on the degree of order in the adsorbed films was obtained from a comparison of the LEED reflection intensities from the test film structure (I) and from an identical thermally-annealed structure (I_{ann}) which was taken to be the most perfect structure. Annealing was implemented by direct incandescent heating of the specimen to the required annealing temperature T_{ann}; the specimen was maintained at this temperature for $t_{ann} = 10$ s after which it was cooled to the bath temperature of the cryomanipulator. When annealing was intended to obtain the most perfect possible film structure, T_{ann} was adjusted to 200–300 K. Below we will argue that the number of structural film defects remaining after this annealing process was negligible. In the kinematic approximation of diffraction theory and neglecting the Debye-Waller effect (which is allowed at low temperatures) we have then $I/I_{ann} = \eta^2$, where η is the order parameter.

We know that if the width of the reflection profile remains unchanged, both the profile amplitude and the integral over the entire profile or over the majority of the profile can be used as a measure of the intensity I. A higher sensitivity of the method is obtained in the second variant, which is used in the present study. Most often the round iris diaphragm of the spot-photometer is set at an aperture dimension d such that only the central portion of the reflection is transmitted to the detector, thereby cutting off the edge near one-half amplitude. Profiles corresponding to different structural states including post-annealing, post-electron-bombardment, and near the order-disorder transition point (Fig. 2) were investigated in order to estimate the error that may result from such integral measurements of I due to possible changes in the profile width from film disordering.

The profiles shown in Fig. 2 were obtained at $d = 0.5$ mm corresponding to a reciprocal-lattice period $\delta k = 1.3 \cdot 10^{-2}$ Å^{-1}. Although this value of δk is comparable to the profile half-width Δk (for example, $\Delta k = 1.5 \cdot 10^{-2}$ Å^{-1} for curve 1) the equipment distortion is not substantial: This is illustrated by curve 7 which shows the corrected I profile (correction by anticonvolution). The difference Δk for curves 1 and 7 is less than 10%. A comparison of the half-width of profiles 1–6 in Fig. 2 shows that the error attributable to the integral measurement of I is less than 5% in investigating the EI disordering and the order-disorder transitions (with the exception of the immediate proximity of the transition point) and therefore can be ignored; in the case of EI ordering the error is greater although in this case it is also possible to bring the error within acceptable bounds by increasing diaphragm size. The background level shown in Fig. 2 is produced by noncoherent quasielas-

tic electron scattering, while the inelastic scattering background is cut off by the four-grid system of the electron diffractometer. The background is identical, within measurement error, for a pure Mo(011) surface and a surface covered by an ordered hydrogen film.

All intensity measurements described in the study were carried out for the first order diffraction reflections on a (2×2) film structure; in an orthogonal coordinate system these reflexes are labeled as (1/2, 1/2). The lowest electron energy levels satisfying the Bragg conditions for successive diffraction by the film and substrate lattices[13] (the corresponding peaks occur at 12 and 20 eV) were used here. Such an energy selection provided a maximum I with a minimum Debye-Waller factor.

Either the same LEED electron gun or different electron guns, one of which (the probe gun) produces a narrower beam, could be used to investigate the EI rearrangement by irradiating the films with electrons in order to alter and probe their structure. Identical results were obtained in both cases. In order to make the probe electron beam have a negligible influence on the structure, in these experiments and other necessary cases I was recorded over a significantly short time period $\Delta t < 1$ s (the variation of I over such a period did not exceed 2%). The absence of any effect on the structure from various light sources, including the gun cathodes, was established independently.

The remaining details of the measurement technique as well as the fabrication of the substrate and the adsorbate sources were identical to those described in previous studies.[5,11]

ATOMIC STRUCTURE AND PHASE TRANSITIONS

In order to obtain submonolayer films the hydrogen was adsorbed when the gas was in disequilibrium with the substrate in an H_2 pressure range $p = 10^{-6}$–10^{-5} Pa at substrate temperatures $T_a = 78$ K and $T_a = 5$ K. A diffraction pattern of the (2×2) structure appears even at a moderate dose of hydrogen molecules directed at the substrate surface, $L = 1.5 \cdot 10^{14}$ cm^{-2}. The change in reflection intensity I of this structure with increasing L is shown in Fig. 3. No other ordered structures nor substrate-reconstruction indicators were observed in the range $L = (0$–$20)10^{15}$ cm^{-2} (as in the case of adsorption of H on W(011), Ref. 14). These observations are consistent with the results of Ref. 12. The (2×2)

pattern vanishes when $L = (6$–$9) \cdot 10^{15}$ cm^{-2} and the (1×1) pattern corresponding to a monolayer is restored. If the hydrogen pressure is maintained at $p > 2 \cdot 10^{-5}$ Pa and the substrate is cooled by liquid helium the background across the entire electron diffractometer screen grows substantially at a large adsorbate dosage $L \geqslant 2 \cdot 10^{16}$ cm^{-2} and the (1×1) pattern vanishes, which can be taken as an indicator of the appearance of a thick amorphous H layer (thicker than a monolayer). Evidently adsorption occurs with the gas and substrate in equilibrium. The subsequent drop in p causes desorption of the thick layer and a restoration of the monolayer (1×1) hydrogen coating. Qualitatively the change in LEED patterns from deuterium adsorption occurs analogously. The same changes in the LEED patterns are observed at equivalent adsorbate doses. No changes were discovered in the work function during the adsorption of H on Mo(011) (within the sensitivity range of the Anderson method: 0.05 eV).

The value of I depends on the annealing, although even without annealing the value of I obtained immediately after adsorption at $T_a = 5$ K is nonzero. A substantial rise in I occurs at $T_{ann} \geqslant 20$ K. The most likely cause of the moderate initial ordering, which is higher for hydrogen than for deuterium, is the rather long-term dissipation of the heat of adsorption of these light adsorbed atoms, during which they can complete several migrational jumps. According to Ref. 15 this time exceeds the oscillation period τ_0 of the H atoms adsorbed on W by two to three orders of magnitude. It is possible to estimate the activation energy of the surface diffusion of the adsorbed atoms from the value to T_{ann} at which I rises most sharply, $T^0_{ann} \approx 60$ K: $E_d \approx k_B T^0_{ann} \ln(t_{ann}/10\tau_0) \approx 0.15$ eV, where k_B is Boltzmann's constant, with 10 migrational jumps assumed to be necessary for substantial ordering.

To establish the nature of the film arrangement we will consider the dependence of the intensity of LEED reflections on concentration. For this purpose it is necessary to convert from the adsorbate dosage L at the substrate surface to the concentration n of atoms adsorbed by the surface. This transformation was carried out by measurements of the thermal desorption (TD) curves[16] at various values of L. To obtain the absolute values of n we utilized a fact established in Ref. 17: A new phase β_1 appears in the TD spectrum of the H–Mo(011) system when $n_{\beta_2} \geqslant 7 \cdot 10^{14}$ cm^{-2}. Figure 3
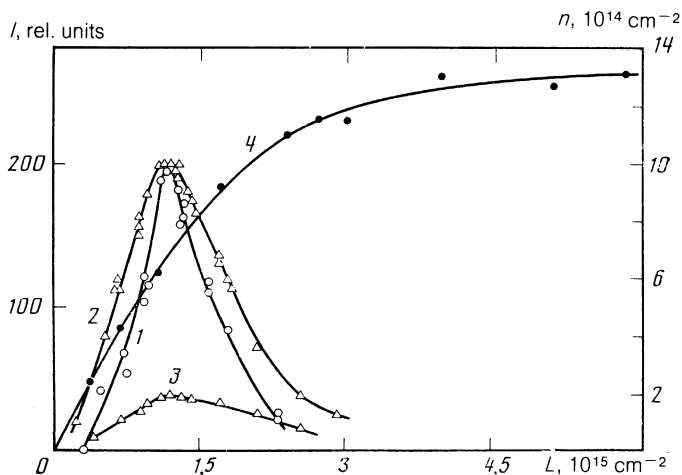

FIG. 3. Intensity I (1–3) of reflections of a (2×2) structure and the concentration n of hydrogen atoms desorbed in the irradiation shot (4) as functions of the adsorbate dosage L applied to the surface at $T_a = 78$ K without annealing (1,4) and at $T_a = 5$ K with annealing (2) and without annealing (3).
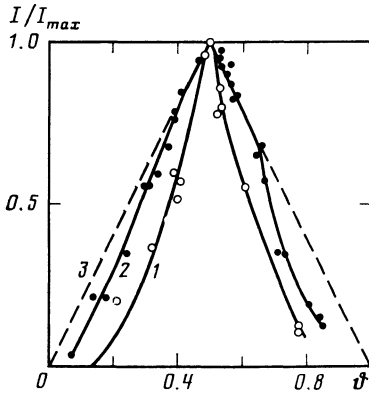
FIG. 4. Reflection intensity of (2×2) structure as a function of hydrogen coverage: 1—$T_a = 78$ K without annealing; 2—$T_a = 5$ K with annealing at $T_{ann} = 200$ K; 3—the expected linear relation $I(\vartheta)$.

FIG. 5. Reflection intensity of the (2×2) structure as a function of temperature for different coverages ϑ: 1—0.18; 2—0.5; 3—0.73.

shows the results from the determination of $n(L)$ at $T_a = 78$ K. It is now possible to plot $I(n)$ based on the $n(L)$ and $I(L)$ data. We shall henceforth use ϑ—the coverage—in place of n for brevity, i.e., the value of n normalized to the concentration of surface substrate atoms $1.43 \cdot 10^{15}$ cm^{-2}. Figure 4 (curve 1) shows such an $I(\vartheta)$ relation corresponding to $T_a = 78$ K. The broad range of the (2×2) structure extending from a value of ϑ near 0 to a ϑ near 1 with an LEED reflection intensity maximum near $\vartheta = 0.5$ indicates the possibility of film growth by means of two first-order phase transitions, a first order phase transition from lattice gas to a (2×2) structure in the range $\vartheta = 0$–0.5, and first order phase transition from a (2×2) to a (1×1) structure near $\vartheta = 0.5$–1. We note that $\vartheta = 0.5$ is stoichiometric for a (2×2) structure not with a primitive cell but rather for a structure containing two adsorbed atoms. We will use a subscript to account for this in the structural designation: $(2 \times 2)_2$. A hypothetical model of this structure is given in Ref. 10.

Assuming that these phase transitions exist and are complete from the kinetic viewpoint we would expect a linear $I(\vartheta)$ relation[18] as shown in Fig. 4 by the dashed line. However the experimental curve in the case $T_a = 78$ K is substantially nonlinear. Possible causes of this deviation include the low order-disorder transition temperature (see below) as well as the elevated level of film dispersion far from the stoichiometric value $\vartheta = 0.5$.

The difference in the values measured at $T_a = 78$ and 5 K of L at which the $I(L)$ curves pass through the maximum is insignificant (see Fig. 2) and this means that similar adsorbate doses are required to obtain coverage of $\vartheta = 0.5$ at both adsorption temperatures, i.e., the adhesion coefficient varies little in the range $T_a = 5$–78 K (at least for $\vartheta \leqslant 0.5$). Hence the same calibration can be used in converting L into n or ϑ in this T_a range. Figure 4 (curve 2) shows the $I(\vartheta)$ relation obtained on this basis from the data in Fig. 3 (curves 2 and 4) for $T_a = 5$ K (with annealing at $T_{ann} = 200$ K prior to measurements of I). A comparison of curves 1 and 2 in Fig. 4 clearly indicates that when $T = 5$ K the experimental $I(\vartheta)$ relation is much closer to a linear relation, suggesting that the assumption of film growth by two first-order phase transitions may be well substantiated. This comparison shows the importance of measuring the LEED intensities at low temperatures. We note that the temperature did not
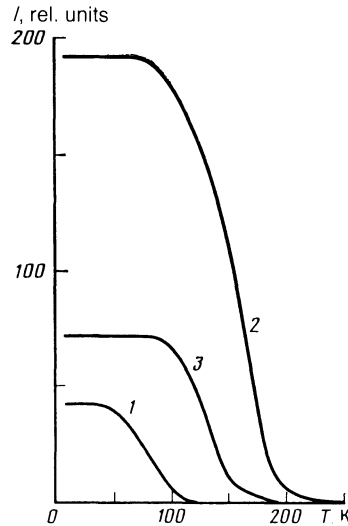
drop below the boiling point of nitrogen in the majority of earlier studies.

The phase diagram was investigated in a higher temperature range by analyzing the order-disorder transitions. The $I(T)$ curves measured with different coatings were used as the raw data. Some of the most characteristic curves are shown in Fig. 5.

Each curve has a broad T range in which $I = $ const on the low-temperature side. A substantial portion of this region lies above the temperature of noticeable surface migration of the adsorbate (20 K, as demonstrated above). Consequently this range of $I = $ const cannot be attributed solely to annealing, and at $T > 20$ K it reflects an equilibrium state with so few defects that they have no effect on the LEED intensity. This fact confirms the previous assumption that a value $\eta = 1$ is attained in the annealed film, at least within the coherence length of the electrons for the LEED technique ($\sim 10^2$ Å).

The high-temperature segments of the curves describe the temperature changes of the order parameter; in the case of second-order transitions such changes occur near the transition temperature T_c and follow the power law[19]:

$$\frac{I(T)}{I_{ann}(T)} = \eta^2(T) = C\left(\frac{T_c - T}{T}\right)^{2\beta}, \qquad (1)$$

where C is a certain constant, while β in the exponent is the index of the order parameter. The method of determining T_c and β is described in detail in Ref. 11. This method is based on an approximation of the experimental $I(T)$ curves by the power law (1). An analysis of the results from processing the curves in Fig. 5 show that the power law holds over a broad range $\Delta T = 30$–50 K which falls 10–15 K short of T_c. The fluctuation process is strongly enhanced in this immediate proximity to T_c; this process causes an additional growth in intensity compared to relation (1). The high-temperature segments of the $I(T)$ curves are therefore in good agreement with the second-order phase transition theory. An investigation of the deuterium films has revealed that the isotope effect does not occur in order-disorder transitions.

It is possible to determine the boundary between the ordered and disordered structural regions on the phase diagram of the H–Mo(011) system based on the derived data with $T_c(\vartheta)$. The overall bell-shaped configuration of our $T_c(\vartheta)$ curve is similar to that measured in Ref. 12. The difference in $T_{c\,max} = 180$ K at $\vartheta = 0.5$ is within the measurement error $(\delta T = \pm 8$K, $\delta\vartheta = \pm 0.05)$. Moreover our $T_c(\vartheta)$ curve is nearly symmetric with respect to the line $\vartheta = 0.5$ while the phase diagram contains two two-phase regions on the low-temperature side in which $(2\times2)_2$ structures coexist with the lattice gas while $(2\times2)_2$ structures coexist with $c(1\times1)$ structures. Our model of a lattice of adsorbed centers in the so-called distorted long bridge positions with repulsion of the first nearest neighbors and attraction of the second nearest neighbors eliminates naturally the difficulties in interpreting the absence of the (2×1) phase at $\vartheta = 0.5$ and explains the two-phase regions of the phase diagram at low-temperatures, unlike the model proposed in Ref. 12 (the long bridge).[20]

The order-parameter exponent β remains constant over a broad range of coatings. The value $\beta = 0.25$ is identical to the value reported in Ref. 11 for the $(2\times2)_3$ structure of H–W(011) which has the same lattice. These values are anomalously high compared to those obtained for other systems although in this case the theory allows anomalous behavior of the exponent β.[21]

ELECTRON-INDUCED REARRANGEMENTS

The perfection of the (2×2) structure is substantially altered under slow electron irradiation. These are nonequilibrium processes; the specimen temperature $T = 5$ K is significantly below the temperature of appreciable thermal migration of the adsorbed atoms, while T remains unchanged during electron irradiation of the specimen. No structural changes in the film will occur over a rather long time period (~ 1 hour) in the absence of an electron beam. Figure 6 illustrates the kinetics of the variation in the reflection intensity I of a stoichiometric (2×2) film irradiated by an electron beam, for two initial film states: after low-temperature adsorption and after annealing. The first of these initial states (prior to electron irradiation) corresponds to a high-
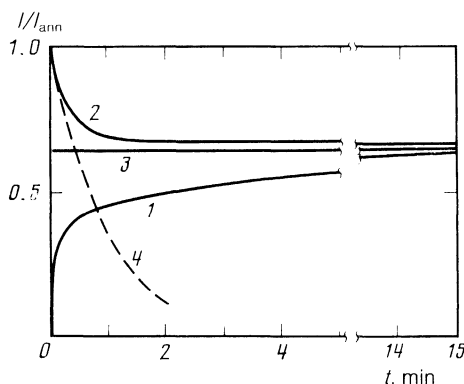
ly-disordered structure, while the second state corresponds to maximum order. The final state is identical in both cases: partial order is established. Partial annealing can be used in the initial state to establish the same degree of order as in the final state for these two cases. The beam induces no changes in I in such a film (curve 3, Fig. 6). The electron beam will therefore induce either order or disorder, depending on the degree of order, while incomplete electron-induced disordering can be attributed to its competing ordering process, which is also electron-induced.

Experiments where the electron current density J_e is varied by a factor of 5 have demonstrated that identical electron doses $J_e t$ will cause identical changes ΔI, while the initial rate of change of I is directly proportional to J_e.

As discussed above, the change of I by electron-induced ordering is accompanied by a substantial rise in the reflection sharpness (see Fig. 2). The half-width Δk diminishes from $3.2 \cdot 10^{-2}$ Å^{-1} (immediately following low-temperature absorption) to $2 \cdot 10^{-2}$ Å^{-1} (following electron irradiation of the same film). Obviously such a film consists of domains substantially smaller than the electron coherence length ($< 10^2$ Å), while the domain dimensions grow during electron-induced ordering. On the other hand the profile width remains unchanged from electron-induced disordering and hence the film state in electron-induced disordering can be described by a model of a lattice containing point defects which, as we know, do not cause broadening of the diffraction reflections.

This model was used previously to determine the electron-induced disordering cross section σ_{EID}.[5,22] However unlike the case of complete EI disordering[5,22] the kinetics of the change of the LEED reflection intensity from both EI ordering and EI disordering of a $(2\times2)_2$ H–Mo(011) lattice is not exponential (compare, for example, curves 2, 4, in Fig. 6). This effect is not due to any electron beam inhomogeneity effects (the result is obtained also when the specimen is irradiated by a broader beam), and in fact reflects the features of opposite electron actions on the structure. An exponential behavior of $I(t)$ normally indicates constancy of the relative rate of change of I remains constant, i.e., of I normalized to unity, which makes it possible to determine the cross section of the process[22]:

$$\sigma_{EID} = \frac{\dot{I}_p(t)}{I_p(t)}\frac{(1-\vartheta)e}{2J_e}, \qquad (2)$$

where e is electron charge. In this case the EI disordering process is accompanied by an inverse ordering process. The rate of the latter will depend on whether the adsorbed atoms occupy the "improper" sites, and hence (2) can be used to determine σ_{EID} only as $t\to0$ when there are still virtually no adsorbed atoms at the "improper" lattice sites. On this basis we obtained a value $\sigma_{EID} \approx 10^{-18}$ cm^2 by reducing curve 2 of Fig. 6. Electron-induced rearrangements are five times slower in deuterium films.

As in the case of the H–W(011) system, electron-induced rearrangements of H on Mo(011) had no kinetic-energy threshold. The variation of I at identical electron irradiation doses (electron energies from $E = 0$ to 30 eV) remains constant to within the measurement error (25%). The zero-threshold effect reported in Ref. 7 can be attributed to the fact that the electrons entering the metal from the

FIG. 6. Kinetics of the variations in reflection intensity of the (2×2) hydrogen structure at $\vartheta = 0.5$ under electron beam irradiation (electron energy $E = 12$ eV) and a current density $J_c = 3\cdot10^{-4}$ A·cm^{-2}. The initial film states: 1—After adsorption at $T_a = 5$ K without annealing (initial value $I/I_{ann} = 0.2$); 2—after annealing at $T_{ann} = 200$ K for 10 s; 3—after annealing at $T_{ann} = 40$ K for 10 s; 4—exponential extrapolation of the initial section of curve 2.

vacuum acquire additional energy equal to the work function Φ (in this case $\Phi = 5$ eV). Hence the energy range from 0 to Φ, in which the threshold of the EI process could be observed in experiments with an external electron source, in concealed. It is only possible to claim that the threshold does not exceed 5 eV in this case.

The set of data on EI rearrangements in ^{1}H and ^{2}H films on the (011) face of Mo (the isotope effect, the weak dependence of the initial rate of electron-induced ordering and disordering on electron energy, and the low energy threshold of the processes) suggests that electron excitation of the adsorbed atoms to the upper-lying vibrational energy levels underlies these processes.[8] As noted above, the quasilocal vibrations of the ^{1}H and ^{2}H adsorbed atoms may be so long-lived that at low temperatures the adsorbed atoms may migrate over substantial distances. Essentially the film is subject to nonequilibrium heating by the electron beam, and the effective temperature T^* may reach tens of kelvins.[8] Then EI ordering is similar to annealing at T^*. Indeed, the potential wells describing the "proper" adsorption centers are $\sim k_B T_c$ deeper than for the "improper" centers. The excited adsorbed atoms will therefore have a higher density of states at the proper centers, meaning that these atoms will most often experience relaxation to the ground state. Moreover the probability of the transition of an adsorbed atom from the lowest level in a deeper well to a level exceeding the surface migration barrier is lower, which also contributes to preferential population of the proper centers. Obviously T^* must not be too high if ordering is to occur. If $T^* > T_c$ EI disordering alone will occur by analogy with the order-disorder transition. In this case $T_c = 100-180$ K and, taking the estimate $T^* < 80$ K[8] into account, the necessary condition $T^* < T_c$ for EI ordering is satisfied.

The long-lived modes in the vibrational excitation spectrum of the ^{1}H and ^{2}H adsorbed atoms apparently plays no small role in the EI ordering process. In order for the adsorbed atom to reach a proper adsorption center on the migration path this path must be of sufficient length. Single jumps of the excited adsorbed atoms to randomly distributed neighboring adsorption centers, which corresponds to disordering, are more probable in the case of long-lived excitations (compared to the vibrational period). This is probably the character of electron-induced disordering in the Li–W(011) system.[22] As to the H–Mo(011) films, both processes must be assumed to exist. In this case the vibrational spectrum of adsorbed H atoms will contain, in addition to the long-lived modes considered in Ref. 8, quite short-lived modes. This is indicated by the simultaneous occurrence of electron-induced ordering and disordering.

[1]R. DiFoggio and R. Gomer, Phys. Rev. Lett. **44**, 1258 (1980).

[2]S. C. Wang and R. Gomer, J. Chem. Phys. **83**, 4193 (1985).

[3]M. Tringides and R. Gomer, Surf. Sci. **166**, 4193 (1985).

[4]A. Auerbach, K. F. Freed, and R. Gomer, J. Chem. Phys. **86**, 2356 (1987).

[5]V. V. Gonchar, Yu. M. Kagan, O. V. Kanash *et al.*, Zh. Eksp. Teor. Fiz. **84**, 249 (1983) [Sov. Phys. JETP **57**, 142 (1983)].

[6]P. P. Lutsishin, O. A. Panchenko, and S. V. Sologub, Poverkhnost'. Fizika, khimiya, mekhanika, No. 8, 22 (1987).

[7]V. V. Gonchar, O. V. Kanash, A. G. Naumovets, and A. G. Fedorus, Pis'ma Zh. Eksp. Teor. Fiz. **28**, 358 (1978) [JEPT Lett. **28**, 330 (1978)].

[8]O. M. Braun and E. A. Pashitskiy, Poverkhnost'. Fizika, khimiya, mekhanika, No. 7, 49 (1984).

[9]R. Liu and G. Ehrlich, Surf. Sci. **119**, 207 (1982).

[10]V. V. Gonchar, O. V. Kanash, and A. G. Fedorus, Pis'ma Zh. Eksp. Teor. Fiz. **38**, 162 (1983) [JETP Lett. **38**, 189 (1983)].

[11]I. F. Lyuksyutov and A. G. Fedorus, Zh. Eksp. Teor. Fiz. **80**, 2511 (1981) [Sov. Phys. JETP **80**, 1317 (1981)].

[12]M. Altman, J. W. Chung, P. J. Estrup *et al.*, J. Vac. Sci. Technol. **5**, 1045 (1987).

[13]P. J. Estrup and E. G. McRae, Surf. Sci. **25**, 1 (1971).

[14]J. W. Chung, S. C. Ying, and P. J. Estrup, Phys. Rev. Lett. **56**, 749 (1986).

[15]O. M. Brachn and E. A. Pashitskiy, Fiz. Tver. Tela (Leningrad) **24**, 1973 (1982) [Sov. Phys. Solid State **24**, 1127 (1973)].

[16]V. N. Ageev and N. I. Ionov, Poverkhnost'. Fizika, khimiya, mekhanika No. 3, 5 (1984).

[17]M. Mahnig and L. Schmidt, Z. Phys. Chem. Neue Folge **80**, 71 (1982).

[18]P. J. Estrup and J. Anderson, Surf. Sci. **8**, 101 (1967).

[19]A. Z. Patashinskii and V. L. Pokrovskii, *Fluctuation Theory of Phase Transitions*, Pergamon, 1979.

[20]K. Binder and D. P. Landau, Surf. Sci. **61**, 577 (1976).

[21]I. F. Lyuksyutov, A. G. Naumovets, and V. L. Pokrovskii, *Two-Dimensional Crystals* [in Russian], Nauk. Dumka, Kiev, 1988.

[22]A. G. Naumovets and A. G. Fedorus, Zh. Eksp. Teor. Fiz. **68**, 1183 (1975) [Sov. Phys. JETP **41**, 587 (1975)].

Translated by Kevin S. Hendzel